


ORIGINAL ARTICLE

Changes in arrhythmogenic properties and five-year prognosis after carbon-ion radiotherapy in patients with mediastinum cancer

Mari Amino MD, PhD¹  | Koichiro Yoshioka MD, PhD¹ | Makiyoshi Shima MD¹ |
Tohru Okada MD, PhD² | Mio Nakajima MD, PhD³ | Yoshiya Furusawa PhD³ |
Shigetaka Kanda MD¹ | Sadaki Inokuchi MD, PhD⁴ | Teruhisa Tanabe MD, PhD⁵ |
Yuji Ikari MD, PhD¹ | Tadashi Kamada MD, PhD³

¹Department of Cardiovascular Medicine, Tokai University, Isehara, Japan

²Department of Radiology, Nagoya University Graduate School of Medicine, Nagoya, Japan

³National Institute of Radiological Sciences, Inage, Japan

⁴Department of Critical Care and Medicine, Tokai University, Isehara, Japan

⁵Ebina General Hospital Cardiovascular Center, Ebina, Japan

Correspondence

Mari Amino, MD, PhD, Department of Cardiovascular Medicine, Tokai University, Shimokasuya 143, Isehara, 250-1193, Japan.
Email: mariam@is.icc.u-tokai.ac.jp

Funding information

KAKEN; Grants-in-Aid for Young Scientific Research (B), Grant/Award Number: 23790880; Tokai University School of Medicine Research Aid

Introduction: Carbon-ion irradiation of rabbit hearts has improved left ventricular conduction abnormalities through upregulation of gap junctions. However, to date, there has been no investigation on the effect of carbon-ion irradiation on electrophysiological properties in human. We investigated this effect in patients with mediastinum extra-cardiac cancer treated with carbon-ion radiotherapy that included irradiating the heart.

Methods and Results: In April–December 2009, eight patients were prospectively enrolled (including two male, aged 72.5 ± 13.0 years). They were treated with 44–72 Gray equivalent (GyE), with their hearts exposed to 1.3–19.1 GyE. High-resolution ambulatory electrocardiography was performed before and after radiotherapy to investigate arrhythmic events, late potentials (LPs), and heart rate variability. Five patients had pre-existing premature ventricular contraction (PVC)/atrial contraction (PAC) or paroxysmal atrial fibrillation (PAF)/AF; after irradiation, this improved in four patients with PVC/PAF/AF and did not deteriorate in one patient with PAC. Ventricular LP findings did not deteriorate and improved in one patient. In eight cases with available atrial LP findings, there was no deterioration, and two patients showed improvements. The low frequency/high frequency ratio of heart rate variability improved or did not deteriorate in the six patients who received radiation exposure to the bilateral stellate ganglions. During the five-year follow-up for the prognosis, six of the eight patients died because of cancer; there was no history of hospitalization for cardiac events.

Conclusion: Although this preliminary study has several limitations, carbon-ion beam irradiation to the heart is not immediately cardiotoxic and demonstrates consistent signals of arrhythmia reduction.

KEYWORDS

arrhythmia, carbon-ion beam, late potential, mediastinum cancer

1 | INTRODUCTION

Carbon-ion (^{12}C) radiation therapy (CIRT) provides an extremely focused form of ionizing radiation that can be delivered to deeply situated targets with little beam entry dose and almost no beam exit dose. Recently, a novel study reported using a carbon-ion beam as an alternative to radiofrequency catheter ablation for the atrioventricular node in Langendorff-perfused porcine hearts (Lehmann et al., 2015). This study demonstrated the feasibility of using a carbon beam scanning with 130 Gy in vivo for atrioventricular node ablation. Based on the results of animal experiments, Constantinescu et al. (2016), developed a clinical study and simulation with nine patients using time-resolved four-dimensional computed tomography (CT) scans to establish the safety and efficacy of CIRT (at ~40 Gy) in a wide-area circumferential ablation for veno-atrial (left atrium-pulmonary vein) junction in hearts with atrial fibrillation. This study considered the toxic energy deposition in the trachea, esophagus, aorta, and phrenic nerves and showed that the use of 25 Gy was safe for all patients. However, using 40 Gy resulted in the projected dose volume limits to the esophagus being reached in three patients, suggesting a potential risk of esophageal perforation.

Since 1999, we have used carbon-ion radiation in animal experiments in Heavy Ion Medical Accelerator at the National Institute of Radiological Sciences in Chiba (HIMAC) for treating ventricular fibrillation in animal models to develop a novel antiarrhythmic treatment (Amino et al., 2006, 2010). Our method is fundamentally different from that of the previous studies (Constantinescu et al., 2016; Lehmann et al., 2015), in which focused ablation with a carbon-ion beam was used to create a block line. The carbon beam was extracorporeally irradiated to the lateral side of the left ventricle (LV), with 15 Gy, not to create a block line but to restore the impaired gap junctions. In the heart, gap junctions constructed from connexins (Cx) provide pathways of intercellular current flow, enabling the propagation of coordinated action potentials and muscle contraction (Severs et al., 2004). We showed that irradiation of rabbit hearts with ^{12}C at 15 Gy improved conduction abnormalities in LVs with myocardial infarction through upregulation of Cx43, but did not result in pathological fibrotic changes (Amino et al., 2006). An improvement in electrical coupling reduced the spatial heterogeneity of repolarization, as well as reducing the vulnerability to fatal ventricular arrhythmias. However, to date, there has been no investigation of electrophysiological properties in human following CIRT, and thus the safety and long-term prognosis of this therapy remains undetermined. In this study, we investigated the electrophysiological effect of carbon irradiation on the heart in patients with mediastinum cancer treated with CIRT.

2 | METHODS

2.1 | Patient population

This study was approved by the Institutional Clinical Ethical Review Board at Tokai University and the National Institute of Radiological Sciences of Japan. Written informed consent was obtained from all subjects prior to study participation.

We prospectively enrolled eight consecutive patients with primary or secondary thoracic malignancy (lung cancer or tracheobronchial adenoid cystic carcinoma) who attended the National Institute of Radiological Sciences for CIRT between April and December 2009. A history of chemotherapy, such as with doxorubicin or fluorouracil, was examined because of the potential for cardiotoxicity, and patients receiving concurrent chemotherapy were excluded. Coexisting cardiac disease and oral medication were investigated before and after CIRT by three cardiologists in Tokai University Hospital via a medical interview, 12-lead electrocardiograms (ECGs), echocardiogram, and high-resolution ambulatory ECG. Oral medications, including antiarrhythmic drugs and beta-blockers, were never changed before and after CIRT to exclude the attributable effects. Follow-up lasted for more than 5 years, during which cancer-related death or history of hospitalization for cardiac events (myocardial infarction, decompensated heart failure, pericarditis, myocarditis, arrhythmia, or sudden cardiac death) was recorded.

2.2 | Irradiation procedure

CIRT was performed in the Charged Particle Therapy Research Center Hospital at the National Institute of Radiological Sciences. The first preparatory procedure to ensure the proper administration of CIRT was fabrication of an immobilization device individual to each patient (Tsuji & Kamada, 2012). This was worn by the patient while a CT scan for treatment planning was obtained. All targets in the mediastinum were extra-cardiac. The target volume was generally determined from CT and positron emission tomography images, in sometimes magnetic resonance imaging was used. Treatment planning for CIRT used the beam-scattering method and the beam-scanning method developed at the Gesellschaft für Schwerionenforschung (Kanai et al., 1980). The initial energy of the ^{12}C beams was 290 MeV/n. Radiation oncologists input contours for target and normal tissue based on the CIRT treatment plan estimated from the CT scans. For all patients, the heart was contoured using a model-based segmentation method that was then adjusted manually to ensure that the entire structure of the heart was encompassed. The whole heart was delineated, along with sub-structures including the chambers, aorta, valves, coronary vessels, pulmonary arteries and veins, and pericardium (Feng et al., 2011; Gomez et al., 2014). At HIMAC, relative biologic effectiveness values of therapeutic carbon beams were determined based on experimental results of cell responses, on values expected with the linear-quadratic model, and based on experiences with neutron therapy. The dose unit in the literature was expressed as Gray equivalent (GyE), which is determined for the clinical situation (Kanai et al., 2006). The data for the carbon beam shown in the table are expressed using GyE.

2.3 | Pre- and posttreatment images

ECG, echocardiogram, and high-resolution ambulatory ECG were performed within a week before CIRT and at 1 month after the final planning of CIRT. The conventional ECG was recorded using a VCM-3000 (Fukuda Denshi, Tokyo, Japan) for the assessment of clinical cardiac

adverse events after cardiac CIRT exposure. Echocardiography was performed to evaluate the thickness of the interventricular septum and LV posterior wall, the LV end-diastolic and end-systolic diameters, the ejection fraction, fractional shortening, early diastole/atrial filling velocity, deceleration time in transmitral flow, regional abnormal wall motion, pericardial effusion, and valve abnormalities. High-resolution ambulatory ECG was performed for the assessment of arrhythmic metrics. The duration of the recording period was 24 hours each time. The equipment employed for high-resolution ambulatory ECG (Spider View, Ela Medical, Paris, France) provided signals at a sampling frequency of 1,000 Hz with 2.5 μV resolution. The signals were acquired using orthogonal X, Y, and Z lead configurations (CC5R, ML, CB2) using standard silver-silver chloride electrodes (Blue Sensor, Linthicum, MD, USA). Analyses were performed at Tokai University. All data were automatically analyzed using commercially available software (Syne SCOPE 3.10) and then confirmed manually by two experienced cardiologists blinded to other clinical observations. The depolarization abnormalities were evaluated from the late potentials (LPs) in the ventricle and atrium, and autonomic balance was examined by analyzing the heart rate variability (HRV).

For the ventricular LP analysis, the QRS wave was added 200 times every 15 min over 24 h. In all of the recordings, three indices of LP were adopted at a noise level $\leq 0.8 \mu\text{V}$: the filtered QRS duration (fQRS), the duration of the terminal low-amplitude signal $< 40 \mu\text{V}$ (LAS40), and the root mean square voltage of the terminal 40 ms of the fQRS (RMS40). The maximal peak fQRS (max-fQRS) and LAS40 (max-LAS40), and the minimal peak RMS40 (min-RMS40), were obtained by selecting the worst values during the 24-h period. LP was considered positive when two of the following three conditions were met: fQRS ≥ 114 ms, LAS40 ≥ 38 ms, and RMS40 $< 20 \mu\text{V}$ (Yoshioka et al., 2013).

The P waves from the orthogonal X, Y, and Z leads were combined spatially into a vector magnitude. The filtered P wave was defined as

signal when showing a persistent level of more than 1 μV and as noise when showing a persistent level of less than 1 μV . The onset and offset of the filtered P wave were determined. Two parameters were assessed via a computer algorithm (Furukawa et al., 2011): the filtered P-wave duration (fPd) and the root mean square voltage of the terminal 20 ms in the filtered P-wave (RMS20). Atrial LP was considered positive when two of the following conditions were met: Ad ≥ 120 ms, and RMS20 $\leq 3.5 \mu\text{V}$.

HRV was analyzed both during the day (8:00–21:00) and at night (23:00–:00). Total power, low-frequency (LF) power, high-frequency (HF) power, and LF/HF were obtained using frequency-domain analysis.

Premature ventricular contraction (PVC) or premature atrial contraction (PAC) was considered clinically significant when the frequency of the episodes of either exceeded 1000/day. Nonsustained ventricular tachycardia was defined as more than three consecutive PVCs sustained for less than 30 s.

3 | RESULTS

3.1 | Patient characteristics and radiotherapy

Background data for the eight subjects enrolled in this study are presented in Table 1. The mean age was 72.5 ± 13.0 years, and six of the eight subjects were women. The underlying diseases were a residual lesion after an operation for tracheobronchial adenoid cystic carcinoma in one subject, primary lung cancer in one subject, metastatic lung cancer in one subject, nodal metastasis after operation of lung cancer in two subjects, and nodal metastasis after the first CIRT for lung cancer in three subjects. For five of the subjects, this was their first treatment with CIRT; the other three had undergone CIRT once before. Three had preexisting cardiac conditions such as paroxysmal

TABLE 1 Backgrounds of patient

Case	Age	Sex	Underlying disease	CIRT in this time	History of cardiac disease	Oral medication for cardiac disease
1	53	F	Residual lesion after operation of TACC	First time	–	–
2	82	F	Primary lung cancer and nodal metastasis	First time	PAF, HT	ARB, beta-blocker
3	84	F	Metastatic lung cancer after operation of colon cancer	First time	–	–
4	55	F	Nodal metastasis after operation of lung cancer	First time	–	–
5	65	M	Nodal metastasis after operation of lung cancer	First time	–	–
6	77	M	Nodal metastasis after CIRT of lung cancer	Second time	–	–
7	80	F	Nodal metastasis after CIRT of lung cancer	Second time	PAF, CHF	Diuretics, pilsicainide, verapamil
8	84	F	Nodal metastasis after CIRT of lung cancer	Second time	HT, CHF	ACE-I, beta-blocker, CCB

CIRT, carbon ion radiotherapy; TACC, tracheobronchial adenoid cystic carcinoma; HT, hypertension; PAF, paroxysmal atrial fibrillation; CHF, chronic heart failure; ARB, angiotensin receptor blocker; ACE-I, angiotensin-converting enzyme inhibitor; CCB, calcium channel blocker.

atrial fibrillation (PAF), hypertension, and chronic heart failure. Oral medication taken by the subjects included angiotensin receptor blockers, beta-blockers, diuretics, pilsicainide, verapamil, angiotensin-converting enzyme inhibitor, and calcium channel blockers. There was no history of catheter ablation for arrhythmia.

The treatment details for the CIRT are listed in Table 2. The targeted lesions were bilateral hilar lymph nodes in one subject, the lateral lung in two subjects, and the superior mediastinal lymph node in five subjects. Of the eight subjects, six received irradiation to the bilateral stellate ganglions. CIRT was conducted with 1–16 fractionated exposures for each subject, with prescribed doses ranging from 44 to 72 GyE. CIRT was inevitably accompanied by irradiation to the heart, including the pulmonary artery, pulmonary vein, aorta, right atrium, left atrium, right ventricle, and LV. The dose delivered to the whole heart ranged from 1.3 to 19.1 GyE. Three cases received direct radiation exposure to the LV (Case 2, 7, and 8). All eight subjects received direct radiation exposure to the pulmonary vein and/or the left atrium.

The subjects were followed up for 5 years, during which time six subjects died from cancer. There was no history of hospitalization for cardiac events.

3.2 | Cardiac CIRT exposure provided no clinical cardiac adverse events

The results of ECG and echocardiogram ensured that the study included patients with actual cardiac exposure; therefore, Case 6 was removed from the analysis ($n = 7$). The prevalence of ECG changes, such as atrioventricular block, abnormal Q waves, poor r wave progression, right bundle branch block, left bundle branch block, and prolonged QTc interval, were all 0% before and after CIRT. However, LV hypertrophy and nonspecific ST-T changes were observed in each subject from the beginning. In the echocardiogram analysis before and after radiotherapy, M-mode tracings were adequate for measuring the interventricular septum (10 ± 0.3 mm vs 10 ± 0.4 mm), LV posterior wall (11 ± 0.3 mm vs 11 ± 0.3 mm), and the LV end-diastolic diameters (46 ± 0.4 mm vs 45 ± 0.4 mm), and end-systolic diameters (32 ± 0.5 mm vs 33 ± 0.4 mm). The wall thickness and LV dimensions did not change with the radiotherapy, and there were no findings of depressed ejection fraction ($59 \pm 6.2\%$ vs $57 \pm 9.1\%$), fractional shortening ($33 \pm 5.5\%$ vs $34 \pm 5.3\%$), or any regional abnormal wall motion. LV hypertrophy was primarily present in one subject, and this did not change with CIRT. The capacity for dilatation was not exacerbated without early diastole/atrial filling velocity >1.5 cm/s (1.0 ± 0.3 vs 1.0 ± 0.3) and deceleration time in the transmitral flow >240 ms (189 ± 20.3 vs 209 ± 17.9). There was no pericardial effusion or valve abnormalities. No subject required additional examination as a result of ECG and echocardiogram abnormalities.

3.3 | Cardiac + stellate CIRT exposure provided improvements in arrhythmia metrics

Ventricular and atrial LPs were evaluated in all patients and summarized in Table 3. High-resolution ambulatory ECG was performed at

TABLE 2 Radiation dose and prognosis

Case	Targeted lesion of irradiation	Fractionated exposure, <i>n</i>	Total dose of CIRT (GyE)	Delivered dose for heart (GyE)						Stellate ganglion (C6/C7) irradiation	Prognosis [M, months after irradiation]
				PA, PV, Ao	RA	LA	RV	LV	LV		
1	Bilateral hilar lymph node (R \geq L)	16	52.8	6.5	5.8	12.2	0	0	0	-	Alive [78 M]
2	Left lung (S8) + left hilar lymph node	1	44	19.1	0	0.7	0.02	4.3	0	-	Cancer death [30 M]
3	Right lung (S6) + superior mediastinal lymph node	16	72	9.1	4.4	11.8	0	0	0	+(R \geq L)	Alive [79 M]
4	Superior mediastinal lymph node (R < L)	12	48	2.9	0	3.1	0	0	0	+(R < L)	Cancer death [51 M]
5	Superior mediastinal lymph node (R > L)	12	48	7.0	3.8	13.4	0	0	0	+(R > L)	Cancer death [63 M]
6	Superior mediastinal lymph node (R = L)	12	48	1.3	0	0	0	0	0	+(R = L)	Cancer death [6 M]
7	Superior mediastinal lymph node (R > L)	12	48	12.3	13.4	14.5	0	0.1	0	+(R > L)	Cancer death [5 M]
8	Superior mediastinal lymph node (R > L)	12	48	12.1	22.6	23.1	0.9	0.1	0	+(R > L)	Cancer death [14 M]

GyE, gray equivalent; S8, anterior basal segment; S6, superior segment of the lower lobe; PA, pulmonary artery; PV, pulmonary vein; Ao, aorta; RA, right atrium; RV, right ventricle; LV, left ventricle; C6/C7, cervical spine 6 and 7; R, right; L, left.

TABLE 3 Ventricular and atrial late potentials

Case	Ventricular late potential						Atrial late potential					
	Before CIRT			After CIRT			Before CIRT			After CIRT		
	fQRS (ms)	LAS40 μ V (ms)	RMS40 ms (μ V)	fQRS (ms)	LAS40 μ V (ms)	RMS40 ms (μ V)	fPd (ms)	RMS20 ms (μ V)	Judgment before and after CIRT	fPd (ms)	RMS20 ms (μ V)	Judgment before and after CIRT
1	88	31	38	86	29	37	126	1.4	(-) \rightarrow (-)	114	7.6	(+) \rightarrow (-)
2	95	35	26	87	30	82	127	4.3	(-) \rightarrow (-)	128	7.0	(-) \rightarrow (-)
3	102	45	10	93	37	22	148	2.8	(+) \rightarrow (+)	139	6.8	(+) \rightarrow (-)
4	107	40	19	101	33	24	116	24.3	(+) \rightarrow (-)	123	4.5	(-) \rightarrow (-)
5	108	35	24	103	26	20	127	9.2	(-) \rightarrow (-)	119	13.5	(-) \rightarrow (-)
6	82	19	127	87	27	84	150	0.4	(-) \rightarrow (-)	147	2.0	(+) \rightarrow (+)
7	79	29	68	84	30	86	NA	NA	(-) \rightarrow (-)	119	3.9	NA \rightarrow (-)
8	150	60	18	149	63	16	155	1.2	(+) \rightarrow (+)	169	3.3	(+) \rightarrow (+)

CIRT, carbon ion radiation therapy; fQRS, the filtered QRS duration; LAS40, the duration of terminal low-amplitude signal <40 μ V; RMS40, the root mean square voltage of the terminal 40 ms of the fQRS; fPd, the filtered P-wave duration; RMS20, the root mean square voltage of the terminal 20 ms in the filtered P wave; (+), positive; (-), negative; NA, not available.

1 month of the last fraction (28 ± 5.7 days). The time from first fraction to the time of examination was 50 ± 15.5 days. Of the eight patients, none had a deterioration of ventricular and atrial LPs. Ventricular LP in Case 4 and atrial LPs in Cases 1 and 3 showed improvement from positive to negative criteria.

The HRV results are summarized in Table 4. LF and HF were extracted during the day and night before and after CIRT, and the variations in LF/HF were analyzed for each individual. The analysis revealed that the LF/HF ratio increased during the day and/or at night in Cases 1 and 2. In six cases with bilateral stellate ganglia exposure (Table 2, Case 3–8), HRV metrics did not deteriorate.

3.4 | Cardiac + stellate CIRT exposure provided arrhythmia reduction

Effects of arrhythmias reduction were evaluated in five cases of patients with pretreatment arrhythmia (Table 5). PVC was observed in two of the patients (Cases 4 and 6); both showed decreased PVC after CIRT. PAC and PAF were observed in three of the patients (Cases 2, 5, and 7). The patient of Case 2 showed the smallest decreasing effect, but the heart exposure to radiation therapy was very small (Table 2, 0.7 GyE to the LA). In the other two cases, PAFs were disappeared. In total, the cases of four patients showed improvement, and none became worse. Representative cases with PVC (Case 4) or PAF (Case 5) are shown in the figures.

3.5 | Case presentation of a subject with arrhythmia reduction

Case 4 was a woman aged 55 years with nodal metastasis after an operation for lung cancer. The patient had no history of arrhythmia screening. Figure 1 shows his delivery dose planning on CT images with a color scale. Transverse views at seven levels corresponding to the dotted arrows in the coronal and sagittal views are shown in the lower panels (Figure 1a to f). Isodose lines on the transverse sections indicate that the left stellate ganglion was exposed to 30% irradiation (green) at the level of the seventh cervical vertebra within the superior margin of the irradiation area (Figure 1a), and the left atrium and left pulmonary vein were exposed to 10% irradiation (violet) within the inferior margin of the irradiation area (Figure 1f). No exposure to the right atrium, right ventricle, or LV was observed in the 12 fractionated exposures. Delivered dose for the heart was 6.0 GyE in total (Table 2).

A virtual 12-lead ECG before radiotherapy obtained by high-resolution ambulatory ECG showed PVC may have occurred from the right ventricle outflow tract (Figure 2a). The quantitative analysis of arrhythmic events before and after irradiation is shown in Figure 2b. Hourly counts of PVC decreased remarkably after irradiation (black bars) in comparison with those before irradiation (white bars). Ventricular LP status changed from positive to negative after radiotherapy (Figure 2c). Figure 3 shows the results of the HRV analysis obtained using the frequency-domain method. Total power and LF and HF power increased during the 24 h after radiotherapy, compared to

TABLE 4 Heart rate variability

Case	Averaged heart rate (bpm)		Before CIRT						After CIRT						Variation of LF/HF before and after CIRT	
	Before CIRT	After CIRT	Daytime			Nighttime			Daytime			Nighttime			Day/Night	
			LF (ms ²)	HF (ms ²)	LF/HF	LF (ms ²)	HF (ms ²)	LF/HF	LF (ms ²)	HF (ms ²)	LF/HF	LF (ms ²)	HF (ms ²)	LF/HF		
1	74	97	250	48	5.23	573	284	2.02	154	21	7.35	58	20	2.93	↑/↑	
2	71	64	1.532	3.562	0.43	195	106	1.85	368	300	1.23	108	143	0.76	↑/↓	
3	78	67	140	31	4.47	352	72	4.88	104	31	3.31	280	290	0.97	↓/↓	
4	63	76	125	24	5.30	99	32	3.08	212	118	1.79	135	142	0.95	↓/↓	
5	66	70	NA	NA	NA	NA	NA	NA	117	23	5.10	243	42	5.84	NA	
6	80	93	19	4	4.49	18	5	3.31	12	4	3.32	16	5	3.20	↓/→	
7	99	78	NA	NA	NA	NA	NA	NA	47	47	0.99	61	68	0.89	NA	
8	70	72	65	82	0.80	71	65	1.09	46	56	0.83	74	70	1.06	→/→	

CIRT, carbon ion radiation therapy; LF, low-frequency power; HF, high-frequency power; NA, not available.

before radiotherapy, whereas LF/HF was relatively decreased. These results were similar in the analyses for both the day and night periods.

Case 5 was a man aged 65 years with nodal metastasis after an operation for lung cancer (Figure 4). The patient suffered from isolated PAF from a year ago but did not desire a treatment with medication or ablation. Isodose lines on the transverse sections indicate that the right stellate ganglion was exposed to ~30% irradiation (*green*) at the level of the seventh cervical vertebra within the superior margin of the irradiation area (Figure 4a), and the left atrium and left pulmonary vein were exposed to ~96% irradiation (*red*) within the inferior margin of the irradiation area (Figure 4f). The right and left atriums and four pulmonary veins were exposed to the irradiation, but neither ventricle was included in the 12 fractionated exposures. Delivered dose for the heart was 24.2 GyE in total (Table 2).

A virtual 12-lead ECG obtained by high-resolution ambulatory ECG revealed PAF before the radiotherapy (Figure 5a). The hourly counts of PAC decreased during the day, and there was no documentation of PAF occurring after the first irradiation (Figure 5b). Although atrial LP status was negative before radiotherapy, the values for two of the LP criteria improved after radiotherapy to within the normal range (the fPd decreased and RMS20 increased) (Figure 5c). The results of HRV analysis are not shown because the analysis was impossible due to the frequent occurrence of PAC and PAF.

4 | DISCUSSION

To the best of our knowledge, this is a first report to detect changes in arrhythmogenic properties after ¹²C irradiation to the heart using ECG, echocardiogram, and high-resolution ambulatory ECG. The main findings were as follows: (1) no clinical cardiac adverse events in the seven subjects with cardiac exposure; (2) ventricular LP findings improved in one subject and did not deteriorate in the other seven; (3) atrial LP findings for the eight subjects showed improvement in two subjects and no deterioration in the other six; (4) the LF/HF ratio of HRV improved or did not deteriorate in the six subjects who received radiation exposure to the bilateral stellate ganglions; (5) in the five subjects with preexisting PVC/PAC or PAF/AF, after irradiation, there was improvement in four patients with PVC/PAF and no deterioration in one patient with PAC; and (6) during the 5-year follow-up, six of the eight subjects died from cancer, and there was no history of hospitalization for cardiac events. However, this study has several limitations such as wide age distribution, various origins of cancer, and spontaneous variability of arrhythmia. Thus, it is difficult to obtain a general conclusion through this preliminary investigation, although it suggests the possibility that CIRT for the heart may indeed even have the potential to ameliorate arrhythmogenesis.

4.1 | Adverse effect by conventional radiotherapy

Thoracic radiotherapy using x-rays or gamma-rays has continued to play an important role in the treatment of lung cancer, Hodgkin's lymphoma, breast cancer, and other malignancies. However, conventional

TABLE 5 Ventricular and supraventricular arrhythmias

Case	PVC count >1,000/day or NSVT			PAC count >1,000/day or PAF		
	Before CIRT	After CIRT	Judgment	Before CIRT	After CIRT	Judgment
1	-	-	-	-	-	-
2	-	-	-	7,045	6,765	No change
3	-	-	-	-	-	-
4	1,848	0	Decreased	-	-	-
5	-	-	-	PAF (+)	PAF (-)	Improve
6	3 run (+)	run (-)	Decreased	-	-	-
7	-	-	-	AF (+)	NSR	Improve
8	-	-	-	-	-	-

CIRT, carbon ion radiation therapy; PVC, ventricular premature contraction; NSVT, non-sustained ventricular tachycardia; PAC, atrial premature contraction; PAF, paroxysmal atrial fibrillation; NSR, normal sinus rhythm.

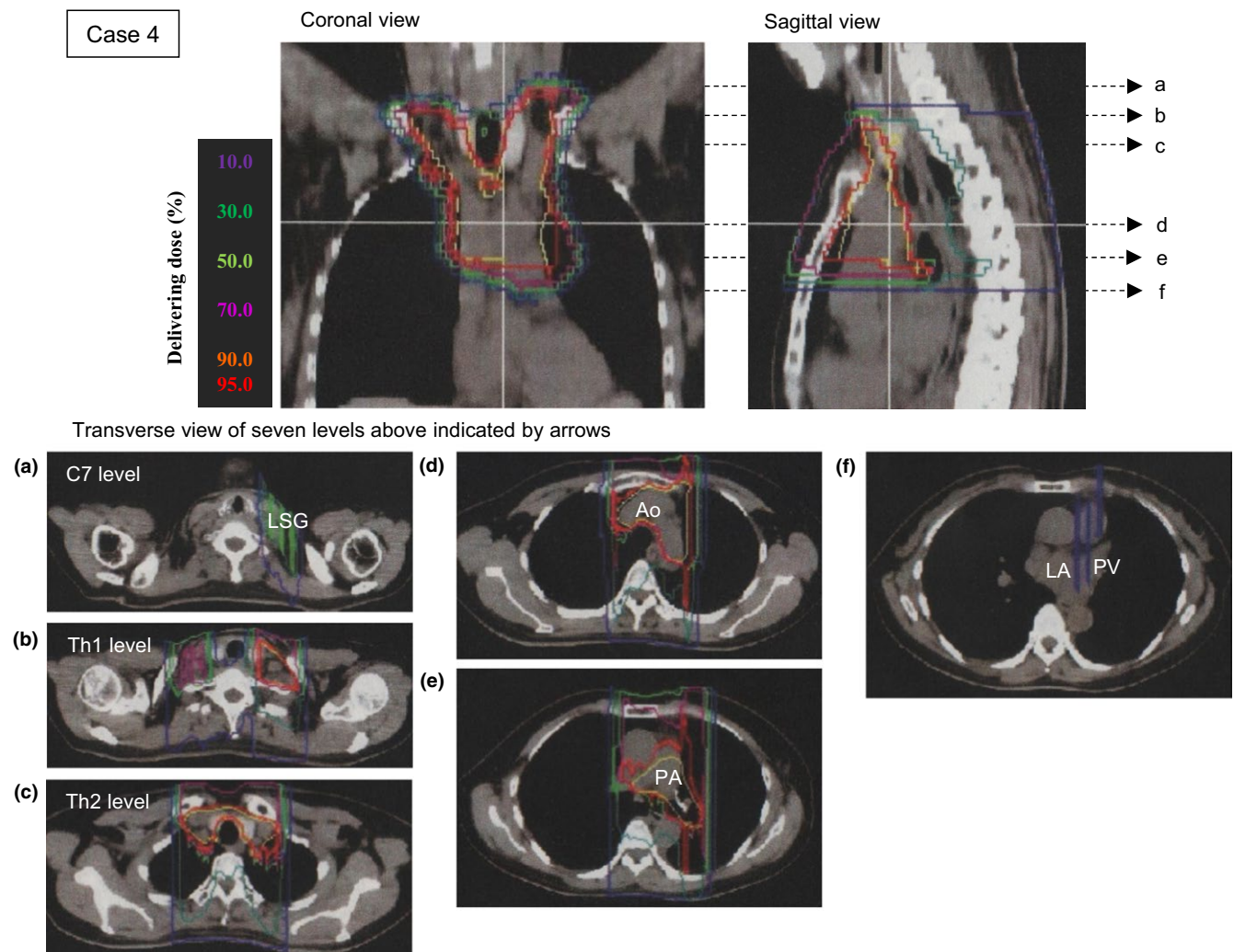


FIGURE 1 Radiotherapy for the superior mediastinum lymph nodes of Case 4 was planned using computed tomography (CT) images. The dose planning images shown are the coronal section, sagittal section, and horizontal section. Six horizontal sections were extracted at the levels of: (a) the seventh cervical vertebra (C7) including the left stellate ganglion (LSG); (b) the first thoracic vertebra (Th1); (c) the second thoracic vertebra (Th2); (d) the aortic (Ao) arch; (e) the pulmonary artery (PA) bifurcation; and (f) the left atrium (LA) with the left pulmonary vein (PV). The estimated delivery dose was drawn on the radiation therapy planning CT images using isodose lines: 10% violet, 30% green, 50% yellow-green, 70% magenta, 90% orange-red, and 95% red

Case 4

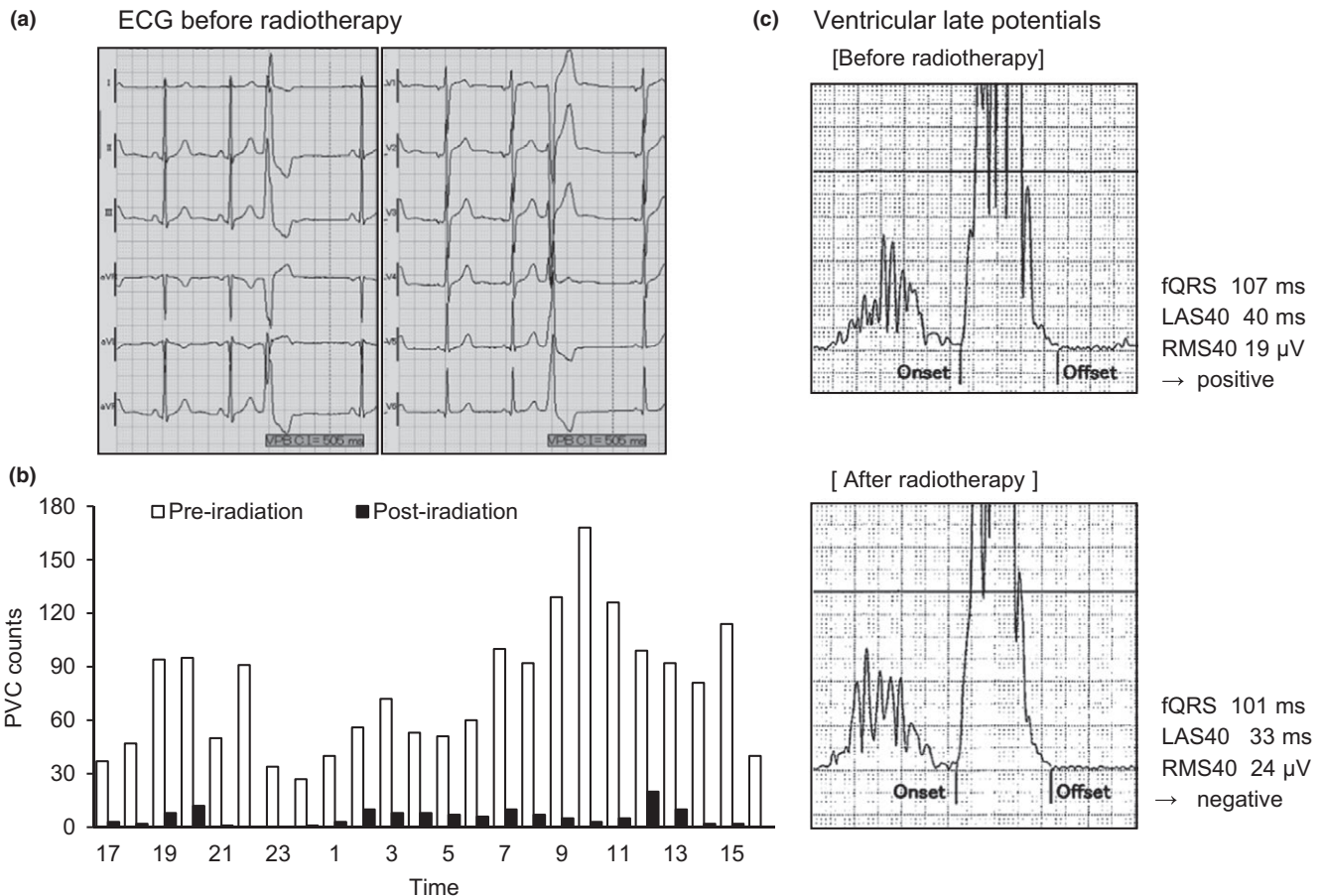


FIGURE 2 Virtual 12-lead electrocardiogram (ECG), frequency graph of premature ventricular contraction (PVC), and trace of ventricular late potential before and after radiotherapy for Case 4. PVC observed on the 12-lead ECG occurred from the right ventricle outflow tract. Hourly counts in the graph showed a remarkable decrease from preirradiation (white bars) to postirradiation (black bars). Three criteria for late potentials are shown: the filtered QRS duration (fQRS); the duration of the terminal low-amplitude signal $<40 \mu\text{V}$ (LAS40); and the root mean square voltage of the terminal 40 ms of the fQRS (RMS40). These criteria changed from positive to negative after carbon-ion irradiation

radiation therapy for the mediastinum has been known to invoke various cardiac diseases. Multiple studies have shown an increased risk of cardiovascular disease, myocardial infarction, valvular heart disease, pericardial disease, heart failure, and sudden death (Aleman et al., 2003; Heidenreich, Hancock, Lee, Mariscal, & Schnittger, 2003).

The myocardium is relatively resistant to the direct effects of radiation because of the lack of myocyte cell division. However, radiation can lead secondarily to reduced myocardial compliance through microvascular insufficiency and ischemia, resulting in varying degrees of diffuse and patchy interstitial fibrosis without an inflammatory reaction (Heidenreich et al., 2003). Alongside the development of morphological damage, hemodynamic studies in various rat strains have revealed a decrease in cardiac output and left ventricular ejection fraction to about 64% of normal values after 20 Gy of radiation (Schultz-Hector, 1992). In the human heart, myocardial fibrosis is usually seen at radiation doses above 30 Gy and is often asymptomatic (Heidenreich & Kapoor, 2009). In one study of 19,063 patients, coronary artery disease developed in 15 patients at a mean of 16 years (range 3–29 years)

after chest irradiation, with a mean dose of 42 ± 7 Gy (McEnery, Dorosti, Schiavone, Pedrick, & Sheldon, 1987). Over the long term, the benefits of radiotherapy for cancer patients may be partially offset by radiation-induced cardiac complications. There is a pressing need to find a way to control thoracic tumors with radiotherapy that is less invasive to the heart and that reduces these risks.

4.2 | Favorable properties of heavy ions

Using charged particle beams such as neutrons, protons, and heavy ions has advantages over conventional radiotherapy (Halperin, 2006). Among these, ions, especially heavy ions such as carbon, provide the advantages and benefits of both neutrons and protons. The fundamental aim when using these beams is to deliver enough energy to kill target cells without causing significant damage to surrounding tissues. Unlike with X-rays, heavy ion beam energy increases with depth penetration up to a sharp maximal point at the end of the range, the so-called Bragg peak. This allows heavy ion beams to deliver a high level

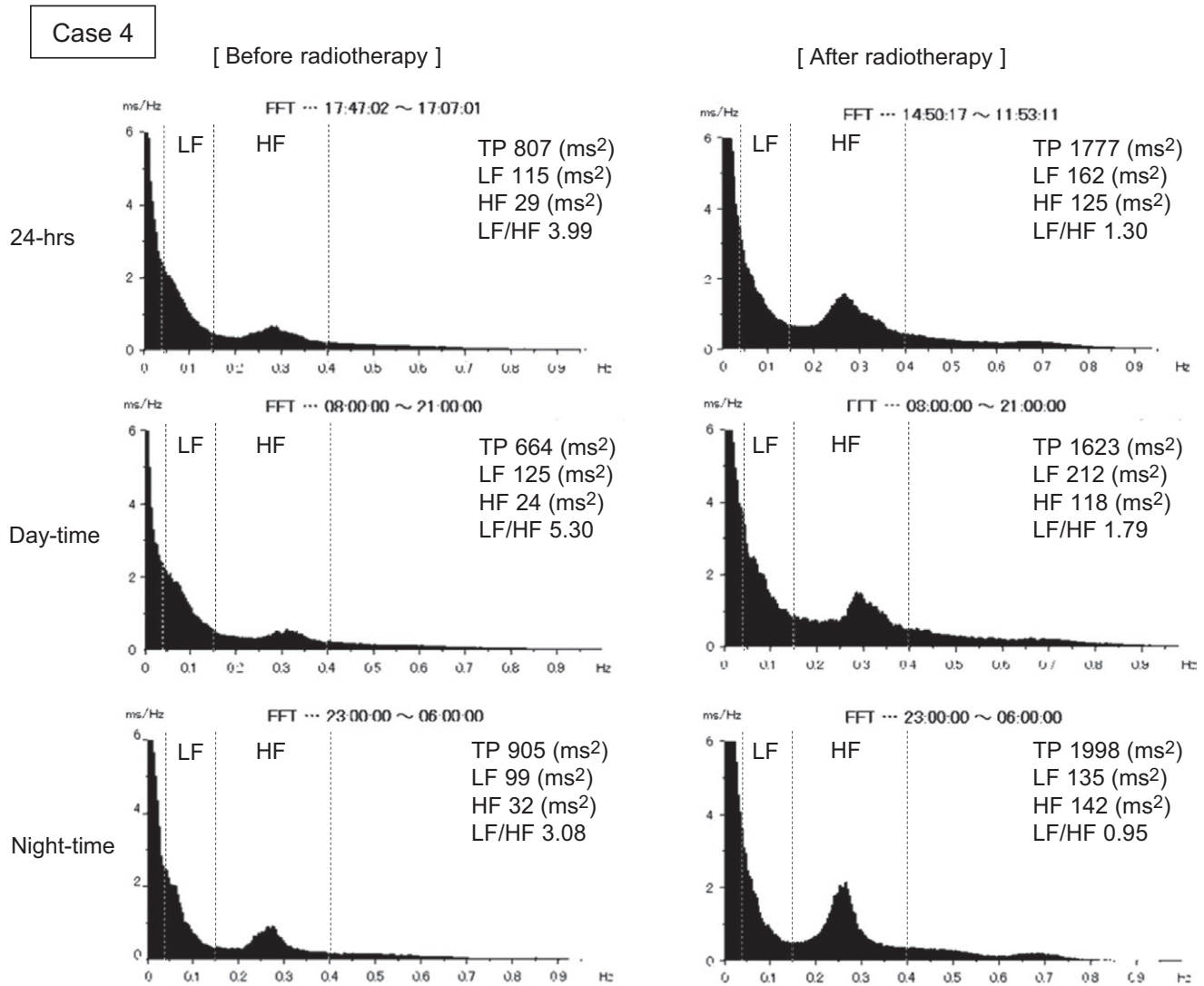


FIGURE 3 Heart rate variability (HRV) analysis in Case 4 using frequency-domain analysis: total power (TP); low-frequency (LF) power; high-frequency (HF) power; and LF/HF during the day (8:00–21:00) and at night (23:00–6:00)

of energy to a focused area and depth. A circumscribed stopping distance, as is the case with protons, is used to achieve highly conformal dose distributions while avoiding an excessive dose to normal tissue uninvolved with tumors. Proton beams also have a Bragg peak, but lateral scatter and misalignment around the target tissue at the beam peak is greater than with carbon beams (Loeffler & Durante, 2013). A high relative biological effectiveness and a low oxygen enhancement ratio, as is the case with neutrons, are considered to be particularly valuable in tackling radiotherapy-resistant tumors.

Since 1994, various trials have investigated the types of tumors that can be effectively treated with ¹²C generated in HIMAC, Japan (Kamada et al., 2015). Most of the patients worldwide who have been cured of cancer by CIRT were treated there; as of February 2016, the institute had treated a total of 9,766 patients with various solid tumors. Carbon-ion beams have also been applied in the treatment of cardiac angiosarcoma and have showed beneficial effects for inhibiting the progression of cancer (Aoka et al., 2004). However, the effects of heavy ions on the heart have not been well characterized during

more than two decades of CIRT. In this study, eight subjects who underwent CIRT and received 1.3–19.1 GyE irradiation to the heart showed no threatening changes in ECGs or echocardiograms or during the five-year follow-up, suggesting the absence of late radiation injury for at least 5 years. A longer follow-up period (more than 10 years) will be needed to assess the occurrence of coronary artery disease and myocardial fibrosis.

4.3 | Electrocardiographic changes after CIRT

Conduction system abnormalities, including various degrees of atrioventricular and bundle branch block, have been reported following heart disease postradiation therapy (Heidenreich & Kapoor, 2009). Although the reported incidence of conduction disease varies, some ECG findings, including repolarization abnormalities and PVCs, can be seen in up to 50% of patients exposed to mediastinal irradiation. Nonspecific ECG abnormalities usually occur in the first year following treatment and are often asymptomatic and transient (Gomez et al.,

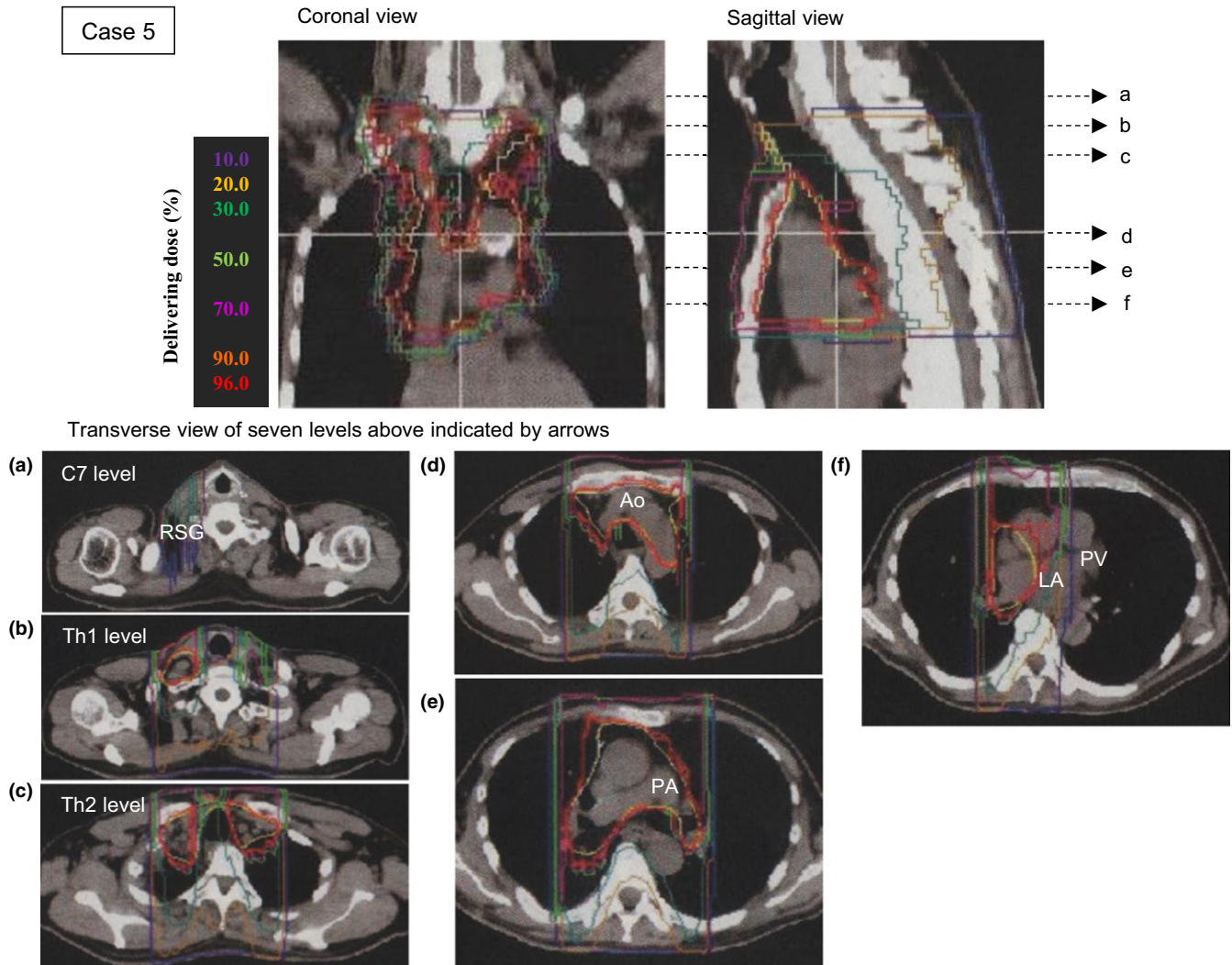


FIGURE 4 Radiotherapy for the superior mediastinum lymph nodes of Case 5 was planned using computed tomography (CT) images. The dose planning images shown are the coronal section, sagittal section, and transverse section. Six transverse sections were extracted at the level of: (a) the seventh cervical vertebra (C7) including the right stellate ganglion (RSG); (b) the first thoracic vertebra (Th1); (c) the second thoracic vertebra (Th2); (d) the aortic (Ao) arch; (e) the pulmonary artery (PA) bifurcation; and (f) the left atrium (LA) with the left pulmonary vein (PV). The estimated delivery dose was drawn on the radiation therapy planning CT images using isodose lines: 10% violet, 30% green, 50% yellow-green, 70% magenta, 90% orange-red, and 95% red

2014). However, these findings were derived from data based on conventional radiation, and there is a lack of information about the effects of heavy ion irradiation.

In this study, there were no conduction abnormalities after CIRT, such as atrioventricular block or bundle branch block. The more prevalent examination in the detection of conduction abnormalities are LPs, which correspond to areas of delayed activation as slowed conduction velocity. LPs are low amplitude, HF electrical signals at the end of ventricle or atrium activation, generated by delayed and fragmented conduction. Ventricular LPs are directly related to the development of ventricular tachycardia or fibrillation (Kuchar, Thorburn, & Samniel, 1986), and atrial LPs are directly related to the AF development (Fukunami et al., 1991). In an investigation of LPs using signal-averaged ECG, it was shown that the heterogeneous Cx43 protein in patients with dilated cardiomyopathy may contribute to impaired

ventricular conduction (Kitamura et al., 2003). Reduced Cx40 levels and heterogeneity of its distribution (relative to Cx43) are commonly observed in AF in the human heart (Gemel et al., 2014). Using Cx40A96S mice as a model for AF showed prolonged P-wave duration and impaired P-wave amplitude (Lübke-meier et al., 2013).

It has recently become possible to continuously record LPs with high-resolution ambulatory ECG (Yoshioka et al., 2013). This has successfully captured LP variability, and has been useful in our investigations for demonstrating that carbon ions did not have an immediate disturbance on electrical conduction systems. We previously reported that a single exposure of the dog heart to ^{12}C irradiation attenuated vulnerability to ventricular arrhythmia after the induction of nontransmural myocardial infarction for at least 1 year, through the modulation of Cx43 expression and LP improvement (Amino et al., 2017). In the case in this study that showed a reduction in PVCs, ventricular LP changed

Case 5

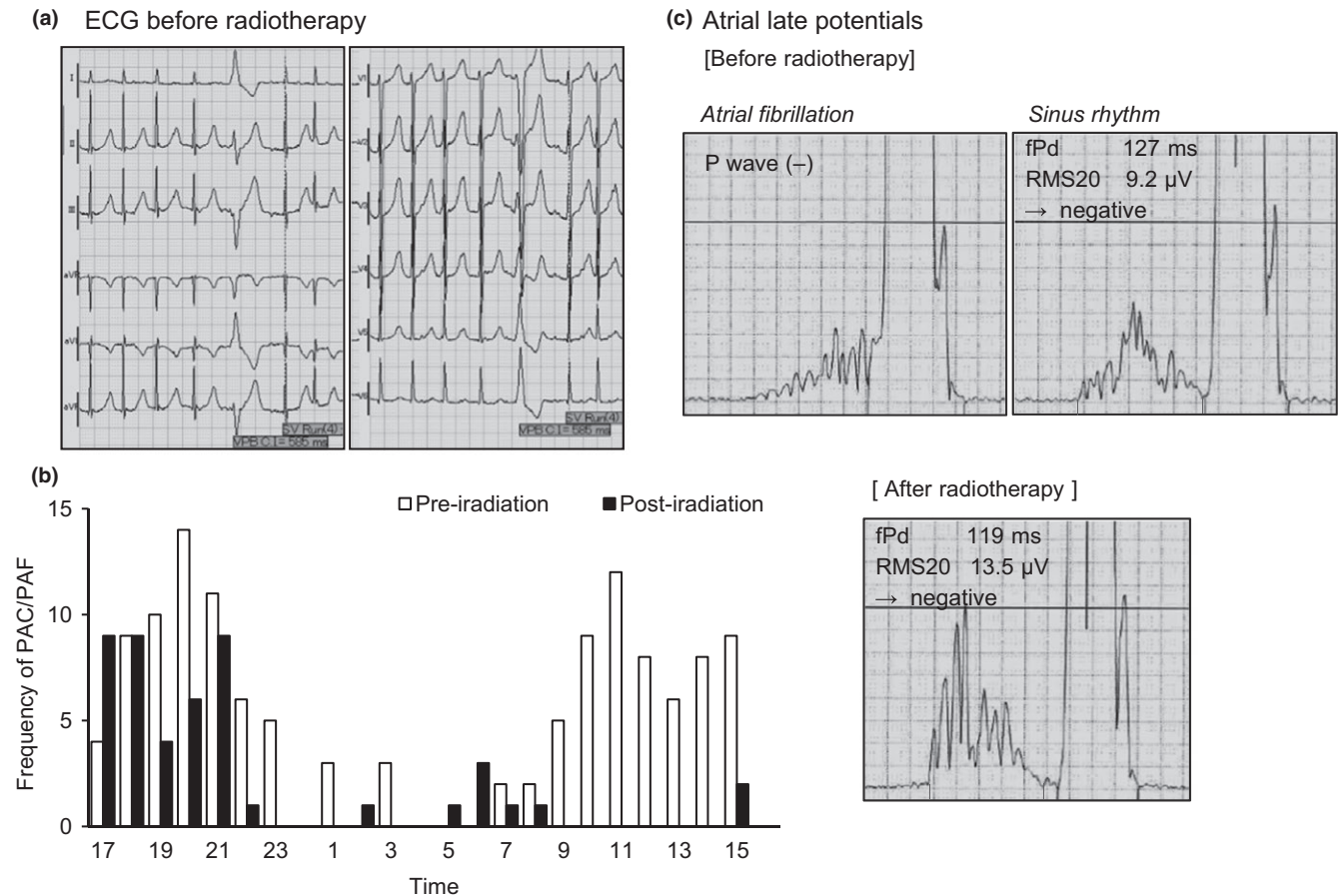


FIGURE 5 Virtual 12-lead electrocardiogram (ECG), frequency graph of premature atrial contraction (PAC) and paroxysmal atrial fibrillation (PAF), and trace of atrial late potential before and after radiotherapy for Case 5. Hourly counts in the graph showed a remarkable decrease from preirradiation (white bars) to postirradiation (black bars) during the day. Two criteria for atrial late potentials are shown: the filtered P-wave duration (fPd); and the root mean square voltage of the terminal 20 ms of the filtered P wave (RMS20). This was negative at baseline, but demonstrated an improvement to within the normal range after carbon-ion irradiation

from the positive to the negative criteria. However, in another four arrhythmic cases, ventricular or atrial LPs were primarily negative or unknown before CIRT. This suggests that an improvement in arrhythmic events may not always correspond with the presence of LPs, but it may be referred from another mechanism such as autonomic balance. There have been many experimental and clinical reports concerning the antiarrhythmic effect of a blockade of the left stellate ganglion for re-entrant fatal tachycardia (Nademanee et al., 2000; Schwartz, Stone, & Brown, 1976). Surgical ablation or regional anesthesia at the left side of the transverse process of the sixth or seventh cervical vertebra is highly selective for inhibiting excessively increased cardiac sympathetic tone, as it decreases heterogeneous repolarization in the ventricles. Bilateral cardiac sympathetic blockade occasionally results in more effects than a unilateral block (Ajjola et al., 2012). Recently, xenon light has sometimes been used instead of anesthetic agents for bilateral stellate ganglions (Nogami & Taniguchi, 2015). However, the usefulness of radiation therapies like xenon light, surgical ablation, or regional anesthesia remains unknown. In this study, four subjects with

good altered arrhythmia received radiation exposure to the bilateral stellate ganglions. Further studies should be conducted to understand the influence and possible efficacy of carbon-ion beams as a sympathetic blockade.

4.4 | Limitations

First, data were only available for eight participants and this small size meant there was little evidence of effect and adverse effect. The post-mortem analysis/pathology was not conducted to determine the adverse cardiac events. Most of them had various origins of cancer and different irradiation targets and dose distributions, thus, making it very difficult to report accurate adverse effects as this largely depends on the dose distribution. This will likely entirely depend on the treatment planning, the respective dose prescriptions and inclusion of risk structures in the target volumes.

Second, the accuracy of P-wave SAEKG would be uncertain when the migration of the sinus or atrial pacemaker is large. Oral medications

would affect heart rate variability, although antiarrhythmic drugs and beta-blockers were never changed before and after CIRT.

Third, the determination of arrhythmias includes the spontaneous variability, and thus, we should also consider other indicators such as T-wave alternans, T-wave variability, heart rate turbulence, and deceleration capacity in the analysis. It is suggested that potential future applications should use high-resolution ambulatory ECG for long-term follow-up, as it is simple and fast for the assessment of proarrhythmia.

5 | CONCLUSIONS

Although this preliminary study has several limitations, it demonstrates the safety of and prognosis after, carbon-ion radiation therapy for patients with mediastinum cancer that included irradiation to the heart. The investigation of LPs using high-resolution ambulatory electrocardiogram could improve understanding of the electrophysiological effects of carbon-ion beams, which might have the potential to improve the management of arrhythmogenesis. Further studies should aim at developing a novel approach using the carbon-ion being available for the treatment of arrhythmia.

ACKNOWLEDGMENTS

We are grateful to the following colleagues for their technical support: Tadashi Hashida and Daisuke Fujibayashi of Tokai University, Takanao Fujii of FUKUDA DENSHI CO., LTD. and Keiko Yamaguchi of Base Line Co., Ltd.

DISCLOSURE

This work was supported by Grants-in-Aid for Young Scientific Research (B) 23790880 from JSPS, and Tokai University School of Medicine Research Aid.

REFERENCES

- Ajjola, O. A., Lellouche, N., Bourke, T., Tung, R., Ahn, S., Mahajan, A., ... Shivkumar, K. (2012). Bilateral cardiac sympathetic denervation for the management of electrical storm. *Journal of the American College of Cardiology*, *59*, 91–92.
- Aleman, B. M., van den Belt-Dusebout, A. W., Klokman, W. J., Van't Veer, M. B., Bartelink, H., & van Leeuwen, F. E. (2003). Long-term cause-specific mortality of patients treated for Hodgkin's disease. *Journal of Clinical Oncology*, *21*, 3431–3439.
- Amino, M., Yoshioka, K., Fujibayashi, D., Hashida, T., Furusawa, Y., Zareba, W., ... Tanabe, T. (2010). Year-long upregulation of connexin43 in rabbit hearts by heavy ion irradiation. *American Journal of Physiology. Heart and Circulatory Physiology*, *298*, 1014–1021.
- Amino, M., Yoshioka, K., Furusawa, Y., Tanaka, S., Kawabe, N., Hashida, T., ... Ikari, Y. (2017). Inducibility of ventricular arrhythmia 1 year following treatment with heavy ion irradiation in dogs with myocardial infarction. *Pacing and Clinical Electrophysiology*, *40*, 379–390.
- Amino, M., Yoshioka, K., Tanabe, T., Tanaka, E., Mori, H., Furusawa, Y., ... Kodama, I. (2006). Heavy ion radiation up-regulates Cx43 and

- ameliorates arrhythmogenic substrates in hearts after myocardial infarction. *Cardiovascular Research*, *72*, 412–421.
- Aoka, Y., Kamada, T., Kawana, M., Yamada, Y., Nishikawa, T., Kasanuki, H., & Tsujii, H. (2004). Primary cardiac angiosarcoma treated with carbon-ion radiotherapy. *The Lancet Oncology*, *5*, 636–638.
- Constantinescu, A., Lehmann, H. I., Packer, D. L., Bert, C., Durante, M., & Graeff, C. (2016). Treatment planning studies in patient data with scanned carbon ion beams for catheter-free ablation of atrial fibrillation. *Journal of Cardiovascular Electrophysiology*, *27*, 335–344.
- Feng, M., Moran, J. M., Koelling, T., Chughtai, A., Chan, J. L., Freedman, L., ... Pierce, L. J. (2011). Development and validation of a heart atlas to study cardiac exposure to radiation following treatment for breast cancer. *International Journal of Radiation Oncology Biology Physics*, *79*, 10–18.
- Fukunami, M., Yamada, T., Ohmori, M., Kumagai, K., Sakai, A., Yamada, T., ... Hoki, N. (1991). Detection of patients at risk for paroxysmal atrial fibrillation during sinus rhythm by P wave-triggered signal averaged electrocardiogram. *Circulation*, *83*, 162–169.
- Furukawa, Y., Yamada, T., Okuyama, Y., Morita, T., Tanaka, K., Iwasaki, Y., ... Fukunami, M. (2011). Increased intraatrial conduction abnormality assessed by P-wave signal-averaged electrocardiogram in patients with Brugada syndrome. *Pacing and Clinical Electrophysiology*, *34*, 1138–1146.
- Gemel, J., Levy, A. E., Simon, A. R., Bennett, K. B., Ai, X., Akhter, S., & Beyer, E. C. (2014). Connexin40 abnormalities and atrial fibrillation in the human heart. *Journal of Molecular and Cellular Cardiology*, *76*, 159–168.
- Gomez, D. R., Yusuf, S. W., Munsell, M. F., Welsh, J. W., Liao, Z., Lin, S. H., ... Grosshans, D. R. (2014). Prospective exploratory analysis of cardiac biomarkers and electrocardiogram abnormalities in patients receiving thoracic radiation therapy with high-dose heart exposure. *Journal of Thoracic Oncology*, *9*, 1554–1560.
- Halperin, E. C. (2006). Particle therapy and treatment of cancer. *The Lancet Oncology*, *7*, 676–685.
- Heidenreich, P. A., Hancock, S. L., Lee, B. K., Mariscal, C. S., & Schnittger, I. (2003). Asymptomatic cardiac disease following mediastinal irradiation. *Journal of the American College of Cardiology*, *42*, 743–749.
- Heidenreich, P. A., & Kapoor, J. R. (2009). Radiation induced heart disease: Systemic disorders in heart disease. *Heart*, *95*, 252–258.
- Kamada, T., Tsujii, H., Blakely, E. A., Debus, J., De Neve, W., Durante, M., ... Chu, W. T. (2015). Carbon ion radiotherapy in Japan: An assessment of 20 years of clinical experience. *The Lancet Oncology*, *16*, 93–100.
- Kanai, T., Kawachi, K., Kumamoto, Y., Ogawa, H., Yamada, T., Matsuzawa, H., & Inada, T. (1980). Spot scanning system for proton radiotherapy. *Medical Physics*, *7*, 365–369.
- Kanai, T., Matsufuji, N., Miyamoto, T., Mizoe, J., Kamada, T., Tsuji, H., ... Tsujii, H. (2006). Examination of GyE system for HIMAC carbon therapy. *International Journal of Radiation Oncology Biology Physics*, *64*, 650–656.
- Kitamura, H., Yoshida, A., Ohnishi, Y., Okajima, K., Ishida, A., Galeano, E. J., ... Yokoyama, M. (2003). Correlation of connexin43 expression and late ventricular potentials in nonischemic dilated cardiomyopathy. *Circulation Journal*, *67*, 1017–1021.
- Kuchar, D. L., Thorburn, C. W., & Samniel, N. L. (1986). Late potentials detected after myocardial infarction: Natural history and prognostic significance. *Circulation*, *74*, 1280–1289.
- Lehmann, H. I., Richter, D., Prokesch, H., Graeff, C., Prall, M., Simoniello, P., ... Packer, D. L. (2015). Atrioventricular node ablation in Langendorff-perfused porcine hearts using carbon ion particle therapy: Methods and an *in vivo* feasibility investigation for catheter-free ablation of cardiac arrhythmias. *Circulation Arrhythmia and Electrophysiology*, *8*, 429–438.
- Loeffler, J. S., & Durante, M. (2013). Charged particle therapy—optimization, challenges and future directions. *Nature Reviews Clinical Oncology*, *10*, 411–424.

- Lübke, I., Andrié, R., Lickfett, L., Bosen, F., Stöckigt, F., Dobrowolski, R., ... Willecke, K. (2013). The Connexin40A96S mutation from a patient with atrial fibrillation causes decreased atrial conduction velocities and sustained episodes of induced atrial fibrillation in mice. *Journal of Molecular and Cellular Cardiology*, *65*, 19–32.
- McEniery, P. T., Dorosti, K., Schiavone, W. A., Pedrick, T. J., & Sheldon, W. C. (1987). Clinical and angiographic features of coronary artery disease after chest irradiation. *American Journal of Cardiology*, *60*, 1020–1024.
- Nademanee, K., Taylor, R., Bailey, W. E., Rieders, D. E., Kosar, E. M. (2000). Treating electrical storm: Sympathetic blockade versus advanced cardiac life support-guided therapy. *Circulation*, *102*, 742–747.
- Nogami, K., & Taniguchi, S. (2015). Stellate ganglion block, compared with xenon light irradiation, is a more effective treatment of neurosensory deficits resulting from orthognathic surgery, as measured by current perception threshold. *Journal of Oral and Maxillofacial Surgery*, *73*, 1267–1274.
- Schultz-Hector, S. (1992). Radiation-induced heart disease: Review of experimental data on dose response and pathogenesis. *International Journal of Radiation Biology*, *61*, 149–160.
- Schwartz, P. J., Stone, H. L., & Brown, A. M. (1976). Effects of unilateral stellate ganglion blockade on the arrhythmias associated with coronary occlusion. *American Heart Journal*, *92*, 589–599.
- Severs, N. J., Copen, S. R., Dupont, E., Yeh, H. I., Ko, Y. S., & Matsushita, T. (2004). Gap junction alterations in human cardiac disease. *Cardiovascular Research*, *62*, 368–377.
- Tsujii, H., & Kamada, T. (2012). A review of update clinical results of carbon ion radiotherapy. *Japanese Journal of Clinical Oncology*, *42*, 670–685.
- Yoshioka, K., Amino, M., Zareba, W., Shima, M., Matsuzaki, A., Fujii, T., ... Tanabe, T. (2013). Identification of high-risk Brugada syndrome patients by combined analysis of late potential and T-wave amplitude variability on ambulatory electrocardiograms. *Circulation Journal*, *77*, 610–618.

How to cite this article: Amino M, Yoshioka K, Shima M, et al. Changes in arrhythmogenic properties and five-year prognosis after carbon-ion radiotherapy in patients with mediastinum cancer. *Ann Noninvasive Electrocardiol*. 2018; 23:e12468. <https://doi.org/10.1111/anec.12468>